

# The Effect of COVID-19 Lockdowns on the Air Pollution of Urban Areas of Central and Southern Chile

## Special Issue:

Special Issue on COVID-19 Aerosol Drivers, Impacts and Mitigation (XVI)

Karina Morales-Solís<sup>1</sup>, Hernán Ahumada<sup>1</sup>, Jhojan P. Rojas<sup>2</sup>,  
Francesco R. Urdanivia<sup>2</sup>, Francisco Catalán<sup>3</sup>, Tomas Claramunt<sup>3</sup>,  
Richard Toro A.<sup>3</sup>, Carlos A. Manzano<sup>3,4</sup>, Manuel A. Leiva-Guzmán<sup>3\*</sup>

<sup>1</sup> Department of Basic Sciences, School of Sciences, Universidad del Bío-Bío, Chillán Campus, Chile

<sup>2</sup> Servicio Nacional de Meteorología e Hidrología (National Meteorological and Hydrological Service), Lima, Peru

<sup>3</sup> Department of Chemistry, Faculty of Sciences, Universidad de Chile, Santiago, Chile

<sup>4</sup> School of Public Health, San Diego State University, San Diego, USA

## ABSTRACT

We present the effects of the confinement and physical distancing policies applied during the COVID-19 pandemic on the concentrations of PM<sub>10</sub>, PM<sub>2.5</sub>, NO, NO<sub>2</sub> and O<sub>3</sub> in 16 cities in central and southern Chile. The period between March and May in 2020 was compared with the corresponding months during 2017–2019, using surface data and satellite information. The relative percent changes in the concentration of atmospheric pollutants, and the meteorological variables observed between these two periods were used to quantify the effects of the lockdowns on the local air quality of the urban areas studied. The results showed statistically significant changes in 11 of the 16 cities. Significant relative changes between +14% and –33% were observed for PM<sub>10</sub> in 9 cities; while statistically significant changes between –6% and –48% were evident for PM<sub>2.5</sub> in 10 cities. Significant decreases between –27% and –55%, were observed in 4 cities in which NO<sub>2</sub> data were available; while significant increases in O<sub>3</sub>, between 18% and 43%, were found in 4 of the 5 cities with available data. The local meteorological variables did not show significant changes between both periods. In all the cities studied, one of the main PM sources is wood burning for residential heating. Although the quarantine imposed during the health emergency could have induced an increase in residential emissions, these were compensated with the reductions in vehicular and/or industrial emissions. Therefore, these results should be carefully interpreted and should inspire new research considering the social, cultural, and economic factors that could alter the common emission patterns and air quality of urban centers.

## OPEN ACCESS

**Received:** December 31, 2020

**Revised:** March 1, 2021

**Accepted:** April 4, 2021

\* **Corresponding Author:**  
manleiva@uchile.cl


**Keywords:** Urban air quality, COVID-19 lockdown, Wood burning emissions, Central and southern Chilean cities

## Publisher:

Taiwan Association for Aerosol  
Research

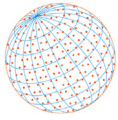
ISSN: 1680-8584 print

ISSN: 2071-1409 online

 **Copyright:** The Author(s).  
This is an open access article distributed under the terms of the [Creative Commons Attribution License \(CC BY 4.0\)](https://creativecommons.org/licenses/by/4.0/), which permits unrestricted use, distribution, and reproduction in any medium, provided the original author and source are cited.

## 1 INTRODUCTION

Air pollution can cause respiratory diseases as a result of chronic (long-term) inflammatory responses (Conticini *et al.*, 2020), short-term respiratory tract irritation (Chen *et al.*, 2020b) and weakening of the natural immune responses, thus making the human body less effective in fighting against diseases caused by viruses (Liu *et al.*, 2019). Previous studies have shown positive associations between Coronavirus disease 2019 (COVID-19) mortality rates (the disease caused by severe acute respiratory syndrome coronavirus 2, SARS-CoV-2) and air pollution (Harapan *et al.*, 2020; Sanità di Toppi *et al.*, 2020; Frontera *et al.*, 2020). Wu *et al.* (2020) found an increase of 8% (95% confidence interval [CI]: 2–15%) in the mortality rate due to COVID-19 with every increase of 1  $\mu\text{g m}^{-3}$  in annual concentrations of PM<sub>2.5</sub> (Wu *et al.*, 2020). Similarly, Ogen *et al.* (2020) showed that



78% of the COVID-19 deaths in France, Spain, Germany, and Italy occurred in areas with greater atmospheric pollution caused by nitrogen dioxide (NO<sub>2</sub>) (Ogen, 2020). These studies showed that the population exposed to higher concentrations of air pollutants, such as PM<sub>2.5</sub> or NO<sub>2</sub>, are more likely to develop clinical complications associated to the SARS-CoV-2 and other respiratory viruses.

On the other hand, the pandemic has resulted in a drastic reduction in global economic activities due to the health policies, physical distancing measures and mobility restrictions implemented worldwide. Quarantines have been applied in countries in all continents as a strategy to minimize the virus transmission rates, and an improvement in local air quality has been reported as a side effect in China (Pei *et al.*, 2020; Zhang *et al.*, 2020), India (Sharma *et al.*, 2020; Shehzad *et al.*, 2020), Europe (Menut *et al.*, 2020), the United States (Chen *et al.*, 2020a), Brazil (Dantas *et al.*, 2020; Nakada and Urban, 2020), Ecuador (Cazorla *et al.*, 2020; Pacheco *et al.*, 2020), and many others, with significant reductions in the concentrations of PM<sub>2.5</sub> and PM<sub>10</sub>, carbon monoxide (CO) and NO<sub>2</sub>. These improvements implied a short-term benefit to human health (He *et al.*, 2020). However, it should be considered that the pandemic hit first the Northern Hemisphere during the transition from winter to spring, which also helped mitigating the effects of air pollution, as well as limiting the meteorological conditions of virus propagation. In the Southern Hemisphere, the outbreak began in late summer and continued during the autumn and winter months, when the worst levels of air quality occur each year (Toro *et al.*, 2014; Molina *et al.*, 2017; Toro *et al.*, 2019). This created a complex scenario, given that in these periods, the emissions produced by residential heating regularly increase and that the meteorological conditions are relatively unfavorable for the natural dispersion of pollutants (Huneus *et al.*, 2020a).

Approximately 60% of the Chilean population (i.e., 10 million people) is exposed to concentrations of particulate matter with aerodynamic diameter less than 2.5 μm (PM<sub>2.5</sub>) that exceed the annual limit of 20 μg m<sup>-3</sup> established by the National Ambient Air Quality Standards (NAAQS) (MMA, 2014). The percent of exposed population will increase if the guidelines of 10 μg m<sup>-3</sup> established by the World Health Organization (WHO) were considered. Moreover, recent estimates made by the Breathelife global campaign for clean air, driven by the WHO, the United Nations Environment Program, and the World Bank, indicated that 6,500 premature annual deaths in 2020 were attributed to air pollution (Breathelife, 2021). Another estimation from State of Global Air 2020 report by the Global Burden of Disease project, produced by the Health Effects Institute (HEI) and the Institute for Health Metrics and Evaluation (IHME), indicated that around 5,900 premature annual deaths were attributable to high PM<sub>2.5</sub> concentrations in Chile during 2019 (SGA, 2020).

The burning of firewood for domestic heating has been identified as one of the main sources of PM<sub>2.5</sub> in the cities of central and southern Chile (Toro *et al.*, 2014; Molina *et al.*, 2017), in which at least 20% of the primary energy consumed comes from firewood (the second most important energy source after oil) (CNE, 2008, 2015). Its widespread use is connected to cultural factors (in the south, heating with firewood is historically associated with the warmth of home), economic factors (firewood is 4 to 7 times cheaper than other sources of energy) and geographical factors (the use of firewood increases in colder and more humid climates) (CNE, 2015; Manzano *et al.*, 2020). However, the long-term exposure to smoke produced by burning wood has been associated with a reduction of lung function, the development of asthma and chronic bronchitis, heart problems and premature mortality; while short term exposures have been associated with acute bronchitis, asthma attacks, worsening of lung diseases and increased susceptibility to respiratory infections (Mead *et al.*, 2018; Cheong *et al.*, 2019; Pani *et al.*, 2020; Punsompong *et al.*, 2021).

In general, the proportion of homes consuming firewood in Chile (with an average national consumption of more than 500.000 m<sup>3</sup> year<sup>-1</sup>) (CNE, 2015), increases with latitude as average daily temperatures decrease (Fig. 1): from ~60% at 34°S (Rancagua) to ~99% at 46°S (Coyhaique). The exception to this trend is the city of Punta Arenas at 53°S, where the availability of natural gas reduces the consumption of firewood to only ~13% of homes (CNE, 2008, 2015). The objective of this study was to characterize the possible changes in the air quality of 16 cities in the central and southern Chile produced by the pandemic prevention and control measures, during a period of the year usually characterized by high air pollution as a result of firewood combustion and adverse weather and geographical conditions. The concentrations of PM<sub>10</sub>, PM<sub>2.5</sub>, nitrogen oxides (NO<sub>x</sub> = NO<sub>2</sub> + NO) and ozone (O<sub>3</sub>) were analyzed by comparing the March–May period of 2020 with the corresponding months of the last three years (period 2017–2019). The effects of the meteorological conditions were also studied.

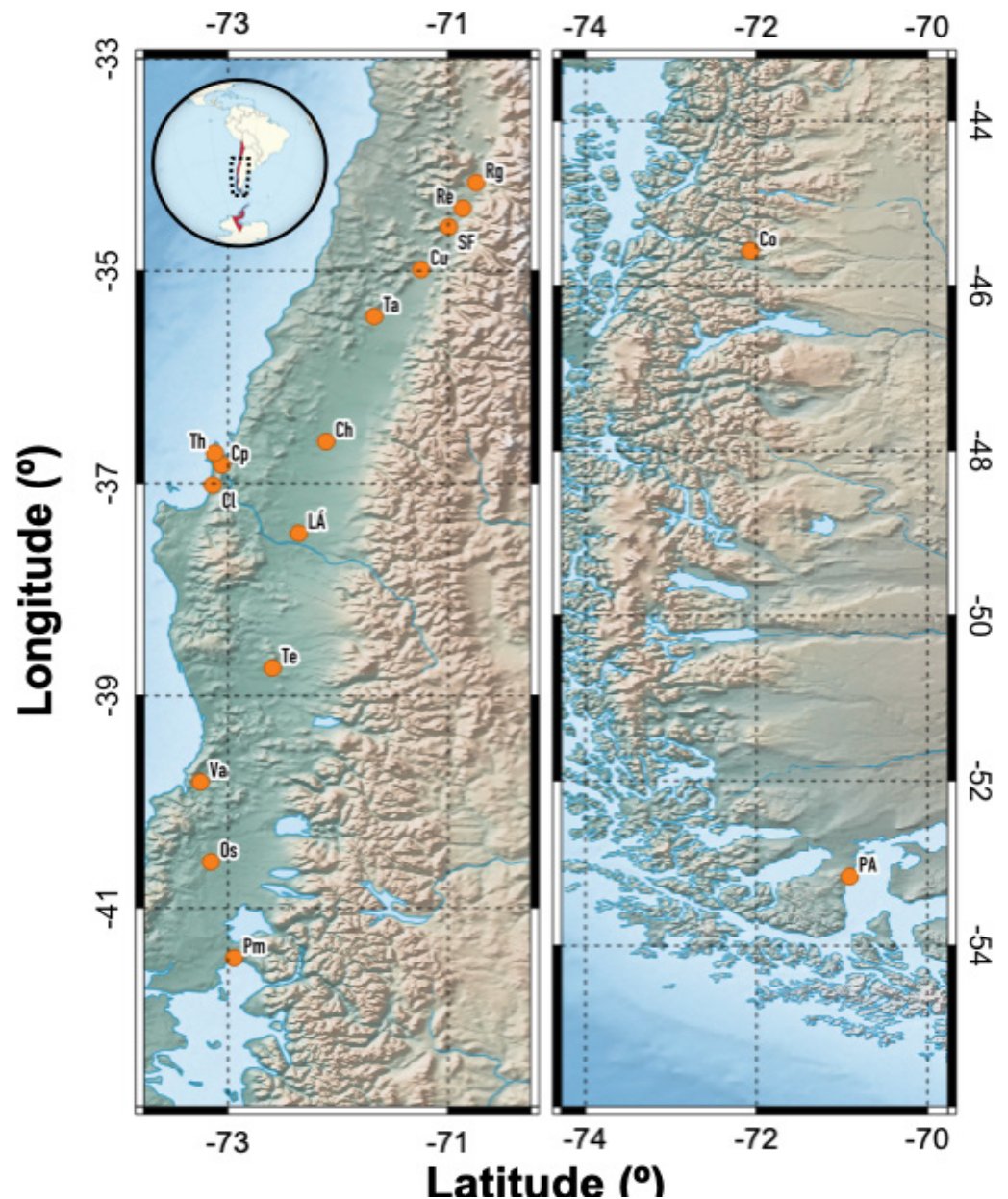
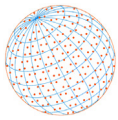


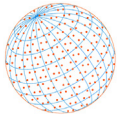
Fig. 1. Locations and IDs of the cities under study. More information is provided in Table 1.

## 2 MATERIALS AND METHODS

### 2.1 Study Area

The study area considered 16 cities at different latitudes of the south-central region of Chile (Fig. 1): Rancagua (Rg), Rengo (Re), San Fernando (SF), Curicó (Cu), Talca (Ta), Chillán and Chillán Viejo (Ch), Los Angeles (LA), Concepción (Cp), Talcahuano (Th), Coronel (Cl), Temuco and Padre las Casas (Te), Valdivia (Va), Osorno (Os), Puerto Montt (Pm), Coyhaique (Co) and Punta Arenas (PA). These cities are not geographically adjacent, thus a potential atmospheric transport among them is negligible, except for Cp, Th and Cl, which are part of a great urban area, (the Great Concepcion). The cities located between 32°S and 38°S (Fig. 1) have a Mediterranean-type climate characterized by a rainy winter period and a dry summer period (IGM, 2013), whereas the cities located between 38°S and 42°S (Fig. 1) have a temperate rainy climate, with frequent rains and lower temperatures than those of the central zone (IGM, 2013). At latitudes further south (> 42°S), the climate becomes colder and is classified as oceanic and tundra. In addition, the Pacific subtropical





anticyclone is present in the region; thus, thermal subsidence inversions occur for much of the year, especially during autumn and winter (Toro *et al.*, 2014, 2019). These overall conditions generate atmospheric stability, which decreases ventilation and promotes the accumulation of pollutants (Díaz-Robles *et al.*, 2014; Toro *et al.*, 2014; Pino *et al.*, 2015).

The cities studied host a total population of approximately 2 million inhabitants (representing 11.7% of the total population, according to the 2010 census) and cover a total area of 658 km<sup>2</sup> (Table 1) (INE, 2020). The largest urban centers studied were Rg, Cp, and Te, with populations between 200,000 and 260,000 inhabitants, followed by Ta, Ch, LA, Va, Os, Pm, PA, Th, Cl, and Cu, with populations between 90,000 and 200,000 inhabitants. Finally, Re, SF, and Co have populations between 30,000 and 50,000 inhabitants.

## 2.2 Surface Measurements

The available hourly air quality data (PM<sub>10</sub>, PM<sub>2.5</sub>, NO<sub>2</sub>, NO, and O<sub>3</sub>) and meteorological variables (temperature (T), relative humidity (RH), wind speed (ws) and direction (wd)) were obtained from the National Air Quality Information System of Chile (SINCA) (Table 1). SINCA is administered by the Chilean Ministry of the Environment through an open online web portal (SINCA, 2020). The data from the 29 monitoring stations in the 16 cities were downloaded from the website in July 2020, validated and analyzed. One city has four monitoring stations (Th), three cities have three monitoring stations (Ta, Cp, and Te), four cities have two monitoring stations (Rg, Ch, Pm, and Co), and the remaining eight cities have only one monitoring station within their urban area (Table 1 and Fig. 1). More information on the instrumentation, location and operation of the monitoring stations can be found in the SINCA website (SINCA, 2020). Briefly, the measurement of the concentration of atmospheric pollutants was carried out using continuous measurement equipment (more details related to station names, measurement principles and instrumentation in SINCA, 2020), with quality control and quality assurance systems to control the flow rate and automatically detecting leaks and identifying instrumental noise. Weekly verifications were performed, and the data were validated to correct for null entries, duplicates and/or other anomalies (SINCA, 2020).

## 2.3 Satellite Information and Remote Sensing

An analysis of the spatial distribution of the levels of the NO<sub>2</sub> tropospheric column was performed using satellite monitoring data. The data were provided by the Copernicus Sentinel-5 Precursor Tropospheric Monitoring Instrument (S5p/TROPOMI), developed by the European Space Agency (ESA), at a spatial resolution of 0.01° × 0.01° and daily temporal resolution (ESA, 2018). The data were downloaded in NetCDF format and then processed in the software R (R Core Team, 2020) and Python (Python, 2020).

## 2.4 Data Analysis

The average concentrations of atmospheric pollutants during 2017-2019 (from March 15 to May 31) were considered as the historical period (HP) and were compared to the concentrations observed in the same period in 2020, the pandemic period (PP). In general, air quality is influenced by short-term local emissions and by synoptic and local meteorological variations with marked diurnal and seasonal variability. Therefore, we reduced the effects of the interannual variability by considering the HP period 2017–2019 for air pollutants and meteorological variables.

The experimental data obtained by the surveillance stations were initially analyzed to identify spurious data. The descriptive statistical analysis of the data was carried out in MS-Excel© software (Microsoft Corporation, Redmond, WA, USA) using the dynamic tables tool and the open source software R (R Core Team, 2020) with the R Studio Environment (R StudioTeam, 2020) and the tool package for air quality analysis for R called OpenAir (Carslaw and Ropkins, 2012; Carslaw, 2019; Carslaw and Ropkins, 2020). The time plots of the hourly averaged concentrations used the local time and average concentrations at the beginning of the hour. The analysis of the variability between both periods (HP and PP) and the calculation of the relative changes expressed as a percentage with respect to the HP period of all the atmospheric pollutants and meteorological variables were used to quantify the effects of the physical distance and confinement measures during 2020 on the air quality of each of the cities.

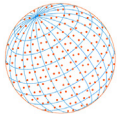
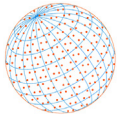


**Table 1.** Monitoring stations studied in central and southern Chile (Fig. 1).

| City         | Region         | City ID | Location (Lat; Lon)  | Population | Area (km <sup>2</sup> ) | Station Name    | Station Location (Lat; Lon) | Measured Variables  |
|--------------|----------------|---------|----------------------|------------|-------------------------|-----------------|-----------------------------|---|
| Rancagua     | VI-O'Higgins   | Rg      | -34.1666°; -70.75°   | 206,971    | 50.36                   | Rancagua 1      | -34.1622°; -70.7139°        | PM <sub>10</sub> , PM <sub>2.5</sub> , T, RH, ws, wd                                      |
|              |                |         |                      |            |                         | Rancagua 2      | -34.1438°; -70.7370°        | PM <sub>10</sub> , PM <sub>2.5</sub> , T, RH, ws, wd                                      |
| Rengo        | VI-O'Higgins   | Re      | -34.4166°; -70.8666° | 30,891     | 9.28                    | Rengo           | -34.3945°; -70.8529°        | PM <sub>10</sub> , PM <sub>2.5</sub> , T, RH, ws, wd                                      |
| San Fernando | VI-O'Higgins   | SF      | -34.5833°; -70.9833° | 49,519     | 12.37                   | San Fernando    | -34.5797°; -70.9896°        | PM <sub>10</sub> , PM <sub>2.5</sub> , O <sub>3</sub> , T, RH, ws, wd                     |
| Curicó       | VII-Maule      | Cu      | -34.9833°; -71.2333° | 93,447     | 20.5                    | Curicó          | -34.9749°; -71.2339°        | PM <sub>10</sub> , PM <sub>2.5</sub> , T, ws, wd  |
| Talca        | VII-Maule      | Ta      | -35.4166°; -71.6666° | 189,505    | 46.04                   | U.C. Maule      | -35.4357°; -71.6195°        | PM <sub>10</sub> , PM <sub>2.5</sub> , T, RH, ws, wd                                      |
|              |                |         |                      |            |                         | La Florida      | -35.4352°; -71.6781°        | PM <sub>10</sub> , PM <sub>2.5</sub> , NO <sub>x</sub> , O <sub>3</sub> , T, RH, ws, wd   |
|              |                |         |                      |            |                         | U. Talca        | -35.4065°; -71.6332°        | PM <sub>10</sub> , PM <sub>2.5</sub> , T, RH, ws, wd                                      |
| Chillán      | XVI-Ñuble      | Ch      | -36.6°; -72.1166°    | 165,528    | 41.03                   | INIA Chillán    | -36.5948°; -72.0893°        | PM <sub>10</sub> , PM <sub>2.5</sub> , T, RH, ws, wd                                      |
|              |                |         |                      |            |                         | Purén           | -36.6162°; -72.0930°        | PM <sub>10</sub> , PM <sub>2.5</sub> , T, RH, ws, wd                                      |
| Concepción   | VIII-Bio Bio   | Cp      | -36.8280°; -73.0513° | 220,803    | 109.5                   | Kingston        | -36.7846°; -73.0520°        | PM <sub>10</sub> , PM <sub>2.5</sub> , NO <sub>x</sub> , O <sub>3</sub> , T, RH, ws, wd   |
|              |                |         |                      |            |                         | ENAP            | -36.7913°; -73.1191°        | PM <sub>10</sub> , PM <sub>2.5</sub> , NO <sub>x</sub> , O <sub>3</sub> , SO <sub>2</sub> |
|              |                |         |                      |            |                         | JUNJI           | -36.7807°; -73.1156°        | PM <sub>10</sub> , PM <sub>2.5</sub> , NO <sub>x</sub> , O <sub>3</sub> , SO <sub>2</sub> |
| Talcahuano   | VIII-Bio Bio   | Th      | -36.7247°; -73.1166° | 92,843     | 92.3                    | C. San Vicente  | -36.7236°; -73.1236°        | PM <sub>10</sub> , PM <sub>2.5</sub> , NO <sub>x</sub> , NO                               |
|              |                |         |                      |            |                         | Indura          | -36.7699°; -73.1138°        | PM <sub>10</sub> , PM <sub>2.5</sub> , NO <sub>x</sub> , O <sub>3</sub>                   |
|              |                |         |                      |            |                         | Inpesca         | -36.7373°; -73.1044°        | PM <sub>10</sub> , PM <sub>2.5</sub>  |
|              |                |         |                      |            |                         | Nueva Libertad  | -36.7361°; -67.1188°        | PM <sub>10</sub> , PM <sub>2.5</sub> , NO <sub>x</sub> , O <sub>3</sub> , ws, wd          |
| Coronel      | VIII-Bio Bio   | Ci      | -37.0166°; -73.2166° | 91,469     | 24.52                   | Cerro Merquín   | -37.0211°; -73.1495°        | PM <sub>2.5</sub> , PM <sub>10</sub>  |
| Los Angeles  | VIII-Bio Bio   | LA      | -37.4666°; -72.35°   | 117,972    | 27.35                   | 21 de Mayo      | -37.4711°; -72.3614°        | PM <sub>10</sub> , PM <sub>2.5</sub> , T, RH, ws, wd                                      |
| Temuco       | IX-Araucanía   | Te      | -38.75°; -72.6666°   | 260,783    | 53.23                   | Las Encinas     | -38.7487°; -72.6207°        | PM <sub>10</sub> , PM <sub>2.5</sub> , T, RH, ws, wd                                      |
|              |                |         |                      |            |                         | Ñielol          | -38.7269°; -72.5798°        | PM <sub>10</sub> , PM <sub>2.5</sub> , T, ws, wd  |
|              |                |         |                      |            |                         | Padre Las Casas | -38.7647°; -72.5987°        | PM <sub>10</sub> , PM <sub>2.5</sub> , NO <sub>x</sub> , T, RH, ws, wd                    |
| Valdivia     | XIV-Los Ríos   | Va      | -39.8138°; -73.2458° | 127,750    | 42.39                   | Valdivia        | -39.8313°; -73.2285°        | PM <sub>10</sub> , PM <sub>2.5</sub> , T, RH, ws, wd                                      |
| Osorno       | X-Los Lagos    | Os      | -40.5725°; -73.1352° | 132,245    | 31.82                   | Osorno          | -40.5844°; -73.1186°        | PM <sub>10</sub> , PM <sub>2.5</sub> , T, RH, ws, wd                                      |
| Puerto Montt | X-Los Lagos    | Pm      | -41.4666°; -72.9333° | 153,118    | 39.58                   | Mirasol         | -41.4795°; -72.9688°        | PM <sub>2.5</sub> , T, RH, ws, wd   |
|              |                |         |                      |            |                         | Alerce          | -41.3991°; -66.8995°        | PM <sub>2.5</sub> , T, RH, ws, wd   |
| Coyhaique    | XI-Aisén       | Co      | -45.5666°; -72.0666° | 44,850     | 18.27                   | Coyhaique 1     | -45.5799°; -72.0610°        | PM <sub>10</sub> , PM <sub>2.5</sub> , T, RH, ws, wd                                      |
|              |                |         |                      |            |                         | Coyhaique 2     | -45.5798°; -72.0499°        | PM <sub>10</sub> , PM <sub>2.5</sub> , O <sub>3</sub> , T, RH, ws, wd                     |
| Punta Arenas | XII-Magallanes | PA      | -53.1666°; -70.9333° | 116,005    | 39.03                   | Punta Arenas    | -53.1583°; -70.9215°        | PM <sub>2.5</sub>   |



### 3 RESULTS AND DISCUSSION

#### 3.1 Concentrations of Atmospheric Pollutants Using Surface Measurements

Fig. 2 shows the mean concentrations for PM<sub>10</sub>, PM<sub>2.5</sub>, NO<sub>2</sub>, NO, and O<sub>3</sub> for the HP (red bar) and the PP (blue bar) and the relative changes between them (light blue bar) for the 16 cities considered in the study. Note that most of the cities studied included PM<sub>10</sub> measurements (13 of 16 cities), and all included PM<sub>2.5</sub> measurements (16 of 16 cities). This is because the PM concentrations in the cities of central and southern Chile frequently exceed the NAAQS in the autumn and winter period of each year (MMA, 2014). For this reason, in the last decade, the Chilean MMA has adopted the policy of expanding the coverage of air quality measurements in these areas by installing monitoring stations with PM measurements in most cities in central and southern Chile. This is not the case for other air pollutants, such as NO<sub>2</sub> and NO, which were measured in only 4 of the 16 cities (Ta, Cp, Th, and Te), while O<sub>3</sub> were measured in 5 of the 16 cities studied (SF, Ta, Cp, Th, and Co). This highlighted the need to expand the coverage of monitoring stations in the country for all criteria pollutants (Toro *et al.*, 2015).

Positive and negative changes were observed when comparing the PM<sub>10</sub> concentrations of the HP and the PP. Positive relative changes of 14%, 12% and 13% were observed in the cities of Re, SF, and Cu, respectively. Changes were not significant in the cities of Va, Rg, Th, and Cp (the 95% confidence level contained 0). On the other hand, the cities of Ta, LA, Ch, Te, Os, and Co showed

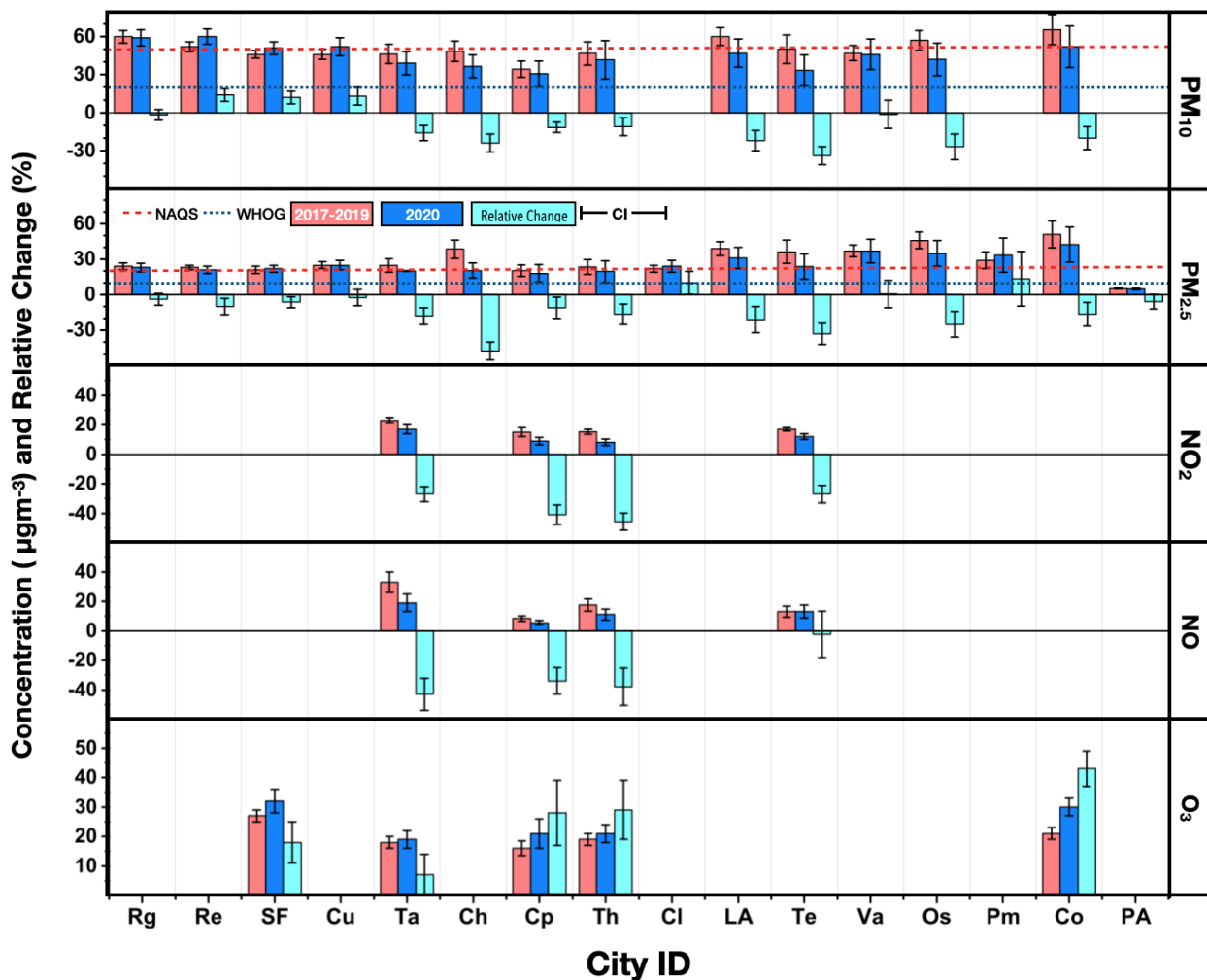
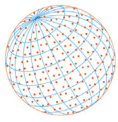


Fig. 2. Concentrations and relative changes in PM<sub>10</sub>, PM<sub>2.5</sub>, NO<sub>2</sub>, NO and O<sub>3</sub> between the historical period (HP: 2017–2019) and the pandemic period (PP: 2020) in the cities studied. Error bars represent the confidence interval of each mean value. NAQS: Chilean national’s air quality standard; WHO: World health organization guideline.



significant decreases of  $-16\%$ ,  $-22\%$ ,  $-24\%$ ,  $-33\%$ ,  $-27\%$  and  $-20\%$ , respectively. Non-significant changes and negative percentage variations were observed for concentrations of  $PM_{2.5}$  (see Fig. 2). Changes were not significant in Va, Rg, Cu, Cl, Pm and PA. Negative relative changes were observed in the cities of Re:  $-10\%$ , SF:  $-6.3\%$ , Ta:  $-18\%$ , Cp:  $-11\%$ , Th:  $-17\%$ , LA:  $-21\%$ , Ch:  $-48\%$ , Te:  $-33\%$ , Os:  $-25\%$  and Co:  $-17\%$ .

In all the cities studied, the PM emissions mainly come from burning wood for residential heating, although there are also other sources, such as vehicle emissions or industries. Therefore, relative changes in ambient concentrations of pollutants could be attributable to changes in the emission patterns induced by the COVID-19 lockdowns, changes in both local (i.e., wind patterns) and synoptic (i.e., thermal inversions) meteorological conditions and nonlinear response of secondary pollutant formation processes due to reductions in precursors ( $PM_{2.5}$  and  $O_3$ ). The cities of Ta, LA, Ch, Te, Os, and Co showed negative relative changes of both  $PM_{10}$  and  $PM_{2.5}$  concentrations attributable to reductions in mobility and non-domestic wood burning resulting in lower emissions of primary PM and gaseous precursors of secondary PM. On the other hand, statistically non-significant changes for both particle fractions were obtained for Va and Rg, where reductions in vehicle emissions driven by the lockdowns were offset by increases in residential emissions from wood burning. Re, SF, and Cu show a particular behavior, with relative increases for  $PM_{10}$  (in the case of Re and SF) and relative reductions for  $PM_{2.5}$ . This behavior could be explained by the secondary character of  $PM_{2.5}$ , whose formation processes would be reduced by decreasing  $NO_x$  emissions from mobile sources (a process that does not affect the coarser PM fractions present in  $PM_{10}$ ).

Significant decreases between the HP and the PP were observed in all cities that registered  $NO_2$  concentrations, ranging from  $-27\%$  to  $-55\%$ . The cities with the smallest changes were Ta and Te, with a value of  $-27\%$ . The highest relative changes were observed in Cp:  $-41\%$  and Th:  $-55\%$ . In the case of NO, the greatest decreases in concentrations were observed in Ta:  $-43\%$ , Th:  $-38\%$ , and Cp:  $-34\%$ . On the other hand, Te did not show significant reductions in the NO concentrations.

The  $O_3$  concentrations during the PP were higher than those during the HP in the five cities where this pollutant was measured. Thus, there were significant increases in the cities of SF:  $18\%$ , Cp:  $28\%$ , Th:  $29\%$  and Co:  $43\%$ . On the other hand, the increase in the  $O_3$  concentration was not significant in the city of Ta. The reasons for this increase and the relative changes of local meteorological conditions that could drive changes in air quality between PP and HP will be discussed in detail later.

### 3.2 Concentrations of Atmospheric Pollutants Using Satellite Measurements

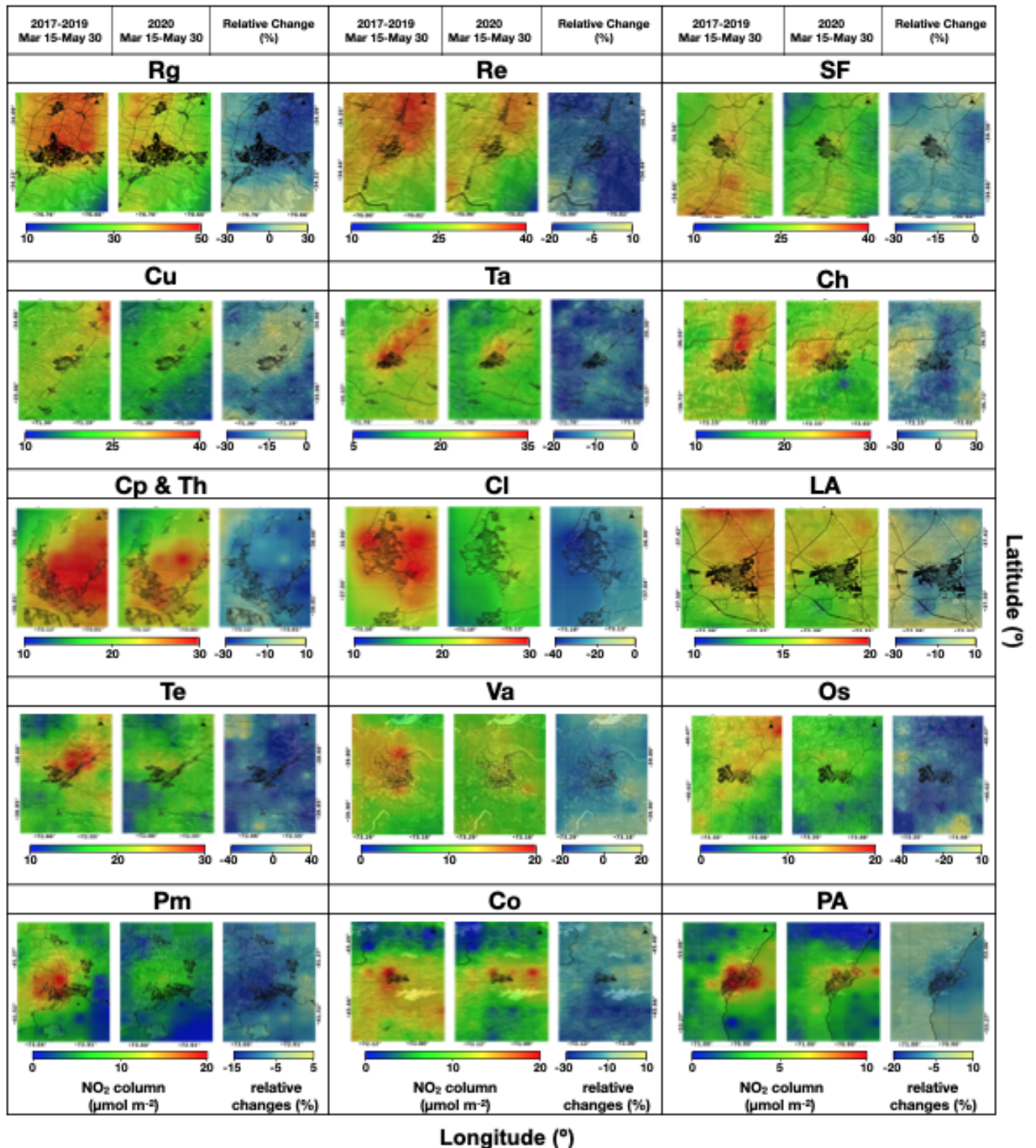
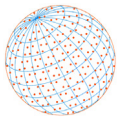
The satellite data were useful for visualizing the impacts of the quarantines applied where surface measurements were not available (ESA, 2018). Additionally, the satellite information allowed the observation of the effects of quarantines on the tropospheric column in the entire urban radius of the most densely populated cities with relatively large vehicle fleets, such as Rg, Ta, Ch, Cp, Th, Cl, Te, Pm, and PA.

Fig. 3 shows the spatial variabilities in the  $NO_2$  column ( $\mu mol\ cm^{-2}$ ) over the selected cities during the HP and the PP, and the percentage relative change between them. The measured values of tropospheric  $NO_2$  in the selected cities were lower in the PP than those in previous years (Fig. 3). The relative changes in the  $NO_2$  tropospheric column were variable, reaching reductions of  $40\%$  in Cl, Te and Os;  $30\%$  in Rg, SF, Cu, Ch, Cp, Th, LA and Co;  $20\%$  in Re, Ta, Va, and PA; and  $15\%$  in Pm, and was not limited to cities with higher population density. The  $NO_2$  concentration reductions observed using surface instruments were consistent with the relative changes observed through satellite information in the cities of Ta, Te, Cp, and Th, although the magnitudes of the changes in Cp and Th were lower.

### 3.3 Contributions of Meteorological Factors and Emission Patterns

The T and RH information was reported in 12 of the 16 cities studied, while the wind speed was reported in 13 of the 16 cities. Fig. 4 shows the mean values of temperature (T), relative humidity (RH) and wind speed (ws) for the HP (red bar), the PP (blue bar) and the observed relative change (light blue bar). In general, there was a slight increase in the mean T in the PP





**Fig. 3.** Spatial variability in the NO<sub>2</sub> column ( $\mu\text{mol cm}^{-2}$ ) over the cities under study for the HP (2017–2019) and the PP (2020) and the relative changes.

compared to the HP, even though this difference was not significant. The exception was the city of Pm, in which a significant decrease in temperature during the PP was observed. Decreases in the RH were observed, although these differences were not significant. A similar result was observed for the wind speed, for which the differences between the periods were not significant. These



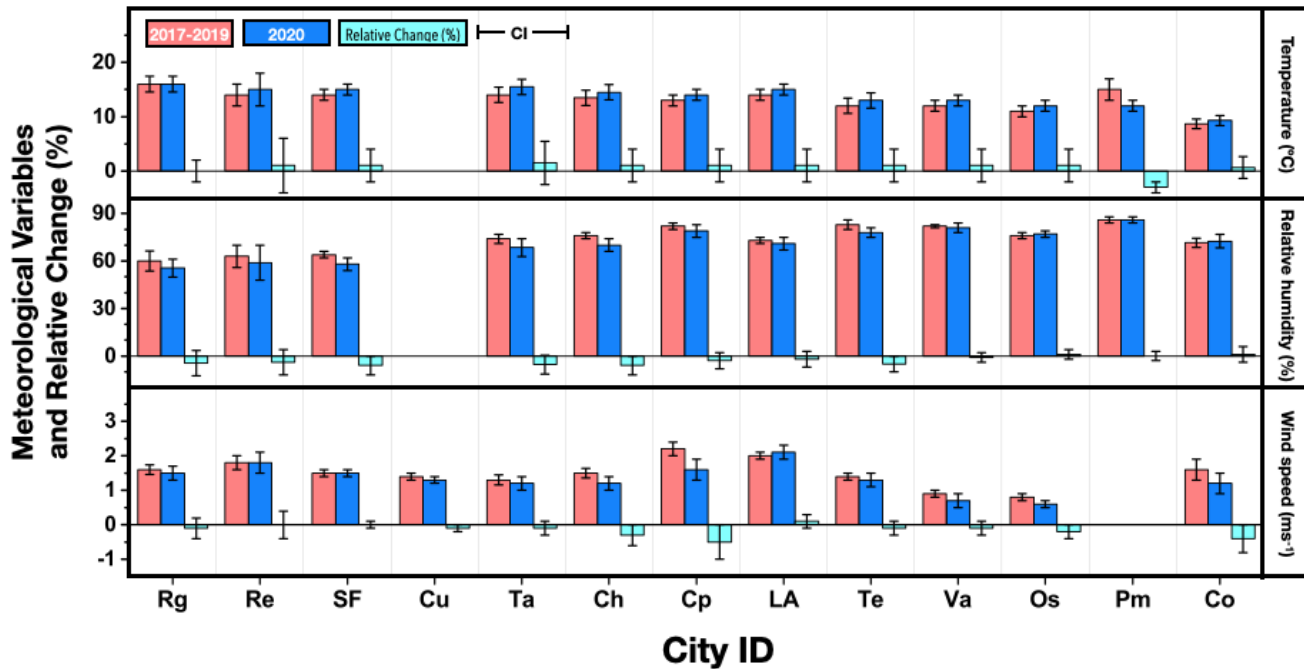
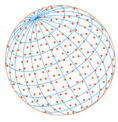


**Fig. 4.** Meteorological variables (temperature, relative humidity and wind speed) and relative changes between the HP (2017–2019) and the PP (2020) in the cities studied.

results established that the changes observed in the concentrations of the air pollutants studied during the HP and the PP were not a product of varying local meteorological conditions. Thus, the changes observed could be attributed to changes in the emission patterns of pollutants as a result of the confinement and physical distancing measures, or to changes in the meteorological conditions on the synoptic scale that cause thermal subsidence inversions. This analysis is beyond the scope of this study.

According to the emission inventories of the 16 selected cities, the largest proportion of emissions is estimated to come from the burning of firewood for residential heating, ranging between 87 and 98% (compared to other sources such as vehicular and industrial emissions), and increasing at higher latitudes (Huneus *et al.*, 2020a; Huneus *et al.*, 2020b). Fig. 5(a) shows this trend through the relationship between annual residential emission rates of PM<sub>2.5</sub> in 2017 and the latitude of the cities under study and their population. The inverse relationship can be explained by the decrease in the average T at more southern latitudes, which implies greater use of firewood as a source of residential heating. The cities of Co and PA are exceptions to the trend shown in Fig. 5(a), the former due to a significantly smaller total population and the latter due to the natural gas subsidized by the state, which means a reduction in the use of firewood for heating.

On the other hand, Fig. 5(b) shows a direct relationship between the annual residential emission rate of PM<sub>2.5</sub> and the PM<sub>2.5</sub>/PM<sub>10</sub> ratio, reaching values above 70% in cities with higher estimated emissions in 2017 such as Te, Va, Os, and Co. Changes in the PM<sub>2.5</sub>/PM<sub>10</sub> ratio between PP and HP allow to identify changes in emission patterns of primary PM and gaseous precursors producing secondary PM. Thus, cities that did not show significant relative changes in PM concentrations nor variations in the PM<sub>2.5</sub>/PM<sub>10</sub> ratio between PP and HP—such as Rg, Cp, and Va, indicate that COVID-19 lockdowns did not affect emission patterns. On the same way, decreases in gaseous precursors of secondary PM were offset by residential firewood burning emissions resulting in non-significant net variations in PM concentrations in the atmosphere. On the other hand, in cities that presented changes in the PM<sub>2.5</sub>/PM<sub>10</sub> ratio between PP and HP, two scenarios can be described. The PM<sub>2.5</sub>/PM<sub>10</sub> ratio decreases during PP, or it increases. The first can be explained by a significant reduction in NO<sub>x</sub> emissions from mobile sources driving decreases in secondary PM<sub>2.5</sub>. This decrease can be offset by an increase in emissions from residential firewood burning due to confinement (this scenario could be the case in cities where Re, Cu, Ta, Th, and Ch). The second scenario occurs in more southern cities such as Os and Co, where the PM<sub>2.5</sub>/PM<sub>10</sub>

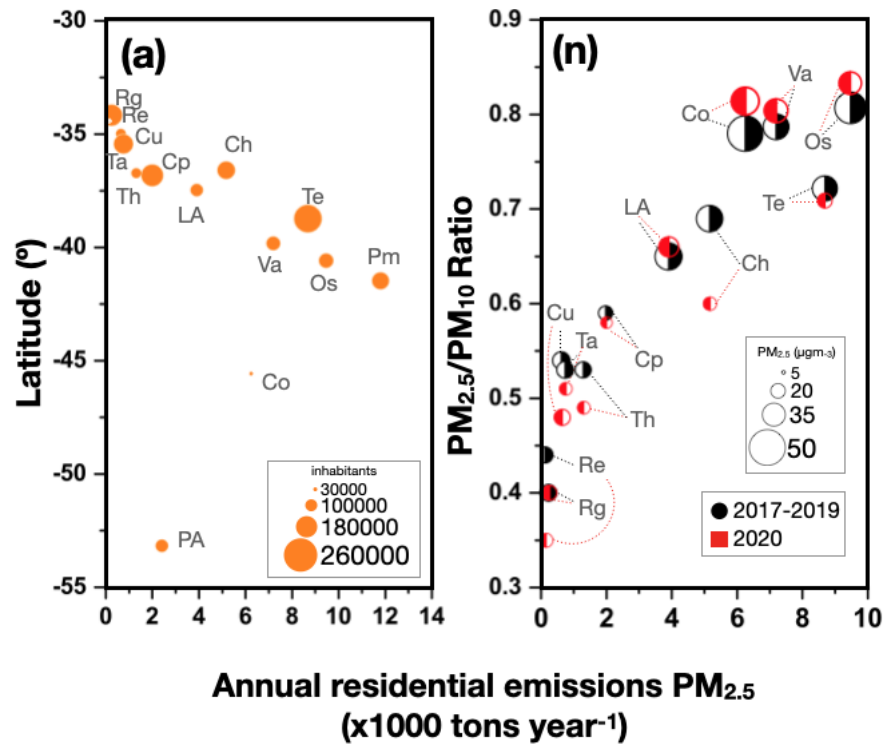
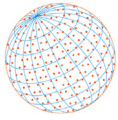
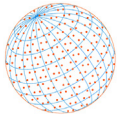


**Fig. 5.** Annual residential emissions of PM<sub>2.5</sub> and their relationship with (a) the latitude of the cities under study and their population and (b) the PM<sub>2.5</sub>/PM<sub>10</sub> ratio and the average concentration of PM<sub>2.5</sub> in PP (2020) and HP (2017–2019) under study.

ratio increased during PP, evidencing the marginal effect that the reduction of emissions from mobile sources in the formation of secondary PM can present in those cities.

Comparing cities, the values observed for the PM<sub>2.5</sub>/PM<sub>10</sub> ratio were consistent with an increase in the proportion of primary emissions from residential firewood burning in southernmost cities. In these cities, the COVID-19 lockdowns could have influenced the pattern of firewood consumption during the PP, which is difficult to quantify. A more detailed analysis to establish how these changes could have altered the pattern of firewood consumption during the PP in each city will be the subject of future research.

Under a global perspective, an increase in O<sub>3</sub> concentrations has been observed in the cities of Rome, Italy (14%) (Sicard *et al.*, 2020), Sao Paulo (30%) (Nakada and Urban, 2020), Barcelona, Spain (43%) (Tobías *et al.*, 2020), Santiago, Chile (63%) (Toro *et al.*, 2021) and Lima, Peru (80%) (Rojas *et al.*, 2021). The production of O<sub>3</sub> depends on a complex and nonlinear tropospheric chemistry between its precursors (VOCs and NO<sub>x</sub>) (Finlayson-Pitts and Pitts, 2000). Thus, under conditions in which the VOC levels are high, but the NO<sub>x</sub> levels are low, the chemistry is “NO<sub>x</sub>-limited”, and more NO<sub>x</sub> implies an increase in O<sub>3</sub> (Finlayson-Pitts and Pitts, 2000). However, under conditions in which NO<sub>x</sub> levels are high, as in many polluted cities around the world, there are “NO<sub>x</sub>-saturated” or “VOC-limited” conditions under which any decrease in NO<sub>x</sub> levels generate an increase in O<sub>3</sub> concentrations (Finlayson-Pitts and Pitts, 2000). Under these conditions, high concentrations of NO<sub>x</sub> serve as a sink for OH radicals, thus a decrease in NO<sub>x</sub> leads to an increase in OH radicals available to react with the VOCs, which promotes an increase in ozone production (Finlayson-Pitts and Pitts, 2000). Additionally, NO reacts rapidly with O<sub>3</sub>, thus a reduction in their concentrations prevents their titration with the consequent accumulation of O<sub>3</sub> (Finlayson-Pitts and Pitts, 2000; Seguel *et al.*, 2020). Therefore, increases in O<sub>3</sub> levels observed during the PP in the cities of central and southern Chile are a direct consequence of the O<sub>3</sub> chemistry. However, the magnitude of the changes in O<sub>3</sub> in a given place are not evident, since they fundamentally depend on the emission rates of the precursors and the amount and the reactivity of the VOCs, as well as the meteorological conditions. Despite this, the results observed in SF, Ta, Cp, Th, and Co establish that these cities are under “NO<sub>x</sub>-saturated” conditions.



### 3.4 Air Pollution and COVID-19 around the World

Fig. 6 shows the relative changes observed in the concentrations of PM<sub>10</sub>, PM<sub>2.5</sub>, NO<sub>2</sub>, and O<sub>3</sub> as a result of COVID-19 prevention and control policies. In general, strict measures have been implemented in almost all countries to contain the spread of COVID-19 disease, which have led to significant changes in air pollution levels in urban areas. The observed changes in atmospheric concentrations of pollutants are variable and depend on the type and timing of restrictions applied in the pandemic period, emission patterns, meteorological variability, geographical conditions and also on the stringency of the measures applied in the PP.

Other cities worldwide have reported reductions in the concentrations of PM<sub>10</sub> and PM<sub>2.5</sub> during the pandemic. The results shown in the Chilean cities is consistent with what has been observed in different cities around the world. In general, these cities implemented pandemic prevention that implied significant reductions in mobility and economic activity, which is mainly associated with vehicular and industrial emissions.

In general, the changes in PM could be explained by variations in primary emissions and/or in the formation of secondary PM. For example, in cities where PM concentrations have increased during pandemic periods, it has been attributed to increased residential wood heating. In addition to primary sources (heating, vehicle exhaust, and industrial activities), numerous secondary sources can also contribute to PM emissions, such as atmospheric photochemical reactions (Huang *et al.*, 2015; Ortega *et al.*, 2016; Sbai and Farida, 2019). The chemistry of the formation of secondary particles is complex. Among the constituents of secondary PM, we find sulfates (formed from the oxidation of SO<sub>2</sub>) (Zhang *et al.*, 2015), nitrates (formed from the oxidation of NO<sub>2</sub>) (Zhang *et al.*, 2015) and secondary organic aerosols (SOA), formed from volatile organic compound (VOC) oxidation (Kroll and Seinfeld, 2008). The rate of formation of secondary organic PM could be enhanced during the closure period due to the increase in O<sub>3</sub> that can be produced by the OH radical in the presence of moisture (Tian *et al.*, 2021). In cities in which concentrations have decreased, they have been affected mainly by vehicle and industrial emissions, which have not been offset by increased emissions from other sources such as residential wood heating or by the formation of secondary aerosols (Tian *et al.*, 2021). Therefore, fine PM levels depend on the emissions of their precursors, which were affected differently by the control policies of the COVID-19 pandemic.

In the case of changes in NO<sub>2</sub> concentrations, reductions are observed in all cities. This would mainly be the result of emission reductions from transport and industrial activities (Bao and Zhang, 2020) led by the restriction of human activities. This behavior is attributed to the drastic decrease in NO<sub>x</sub> levels, leading to the reduction of O<sub>3</sub> consumption by NO (Sharma *et al.*, 2020). In addition, in rural areas it could be explained by the increase of O<sub>3</sub> resulting from air mass transport.

## 4 CONCLUDING REMARKS

This study establishes the effect of confinement and physical distancing measures in the context of the COVID-19 pandemic on PM<sub>10</sub>, PM<sub>2.5</sub>, NO, NO<sub>2</sub>, and O<sub>3</sub> pollutant concentration levels in central and southern Chile cities. The reduction in emissions has not automatically led to a decrease in air pollutant concentrations at COVID-19 times, as the concentration of pollutants in the air is affected by a variety of complex factors.

Statistically significant relative changes in PM<sub>10</sub> and PM<sub>2.5</sub> concentrations during the PP with respect those during the HP were observed in 9 and 10 cities, respectively. In all the cities under study, the PM emissions mainly come from burning wood for residential heating. The changes in the emission patterns induced by the COVID-19 pandemic in these cases were not clear because the confinement measures could have induced an increase in the residential emissions, and a reduction in vehicular and industrial emissions. Additionally, the possible variations in the environmental conditions on the synoptic scale can also affect the dispersion of pollutants in each city. The results of both remote sensing and surface measurements showed significant reductions in NO<sub>2</sub> concentrations during the PP. In the case of O<sub>3</sub>, significant increases are observed in 4 of the 5 cities studied. These increases are associated with changes in the concentrations of NO<sub>x</sub>, since the cities were under "NO<sub>x</sub>-saturated" conditions. These results include only 5 cities, highlighting the need to expand the coverage of air quality stations in the country.

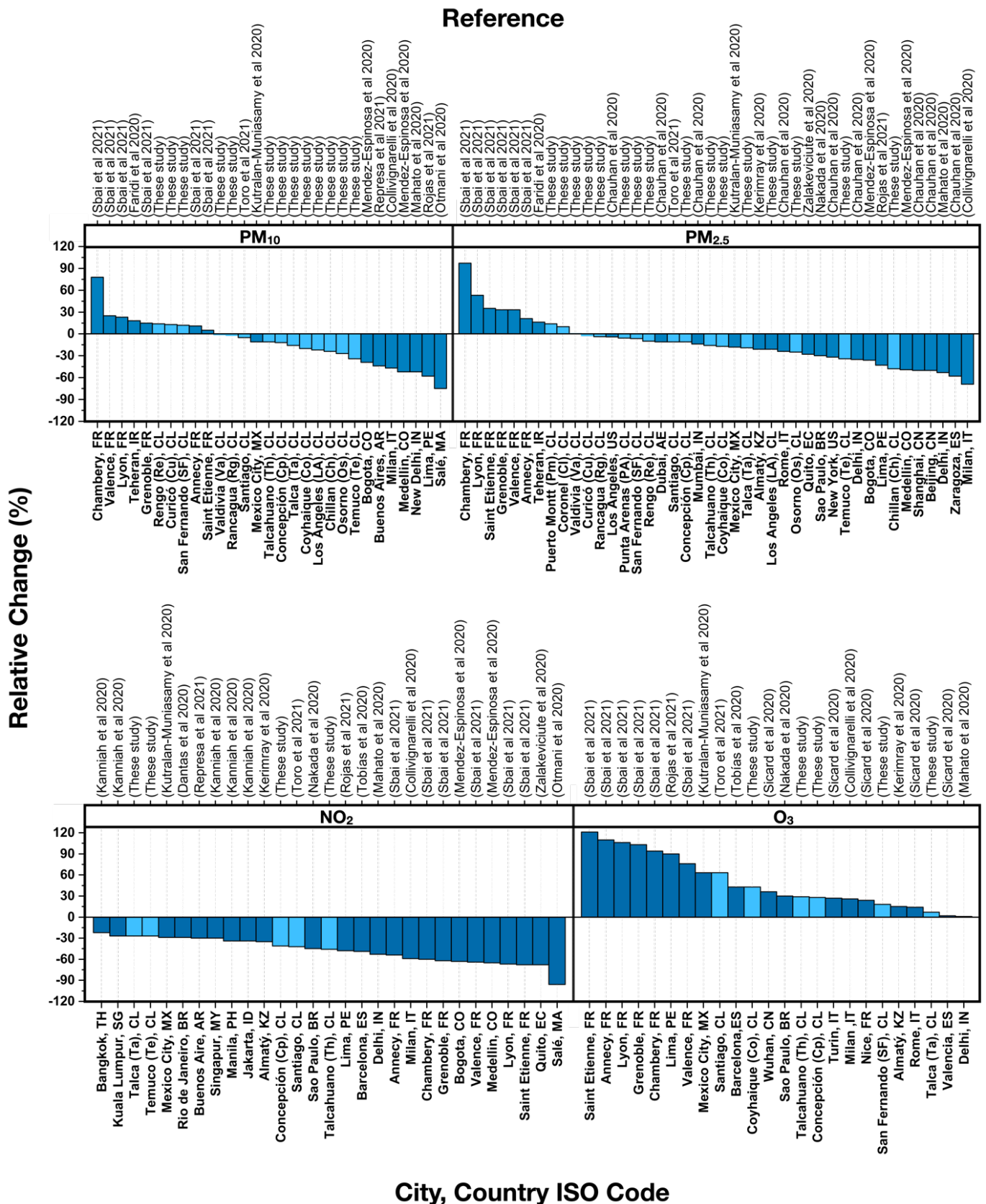
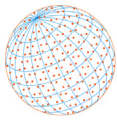
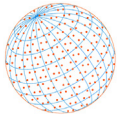


Fig. 6. Comparison of relative changes in the concentration of atmospheric pollutants due to countermeasures against COVID-19 in cities around the world (Chilean cities in light blue).





Finally, the results presented should be interpreted with caution and should inspire new research that considers a longer period of time, a detailed study of the emission patterns in each city and the social, cultural and economic factors that could induce changes in the emission patterns, and their consequent effect on air quality will allow us to evaluate control measures and strategies for the prevention of air pollution and at the same time review the quality of the emission inventories of the cities under study.

## ACKNOWLEDGMENTS

---

We acknowledge partial support from National Research and Development Agency, Chilean Government ANID/FONDECYT 2020 grant no. 1200674, ANID/FONDEQUIP grant no. EQM190045 and Servicio Nacional de Meteorología e Hidrología del Perú (SENAMHI-Perú) for project SNIP N° 199842 “Extension and improvement of the monitoring network for the forecast of air quality in the metropolitan area of Lima” and program 096 (PPR096) - Management of air quality.

## DISCLAIMER

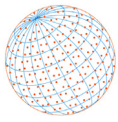
---

The authors declare that they have no known competing financial interests or personal relationships that could appear to influence the work reported in this paper.

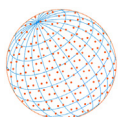
## REFERENCES

---

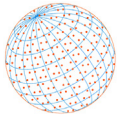
- Bao, R., Zhang, A. (2020). Does lockdown reduce air pollution? Evidence from 44 cities in northern China. *Sci. Total Environ.* 731, 139052. <https://doi.org/10.1016/j.scitotenv.2020.139052>
- Breathelife (2021). The Air Pollution in Santiago Chile. [https://breathelife2030.org/city\\_data/santiago/](https://breathelife2030.org/city_data/santiago/) (accessed 25 February 2021).
- Carslaw, D. (2019). The Openair Manual Open-Source Tools for Analysing Air Pollution Data, Version: 12th November 2019. University of York and Ricardo Energy & Environment. <https://bit.ly/2zldmMO> (accessed 15 March 2020).
- Carslaw, D., Ropkins, K. (2020). Openair: Tools for the Analysis of Air Pollution Data, R Package Version 2.7.2. The Comprehensive R Archive Network (CRAN). Package openair - R Project, <https://bit.ly/2SsoPXm> (accessed 15 March 2020).
- Carslaw, D.C., Ropkins, K. (2012). *openair* — An R package for air quality data analysis. *Environ. Modell. Software* 27–28, 52–61. <https://doi.org/10.1016/j.envsoft.2011.09.008>
- Cazorla, M., Herrera, E., Palomeque, E., Saud, N. (2020). What the COVID-19 lockdown revealed about photochemistry and ozone production in Quito, Ecuador. *Atmos. Pollut. Res.* 12, 124–133. <https://doi.org/10.1016/j.apr.2020.08.028>
- Chen, L.W.A., Chien, L.C., Li, Y., Lin, G. (2020a). Nonuniform impacts of COVID-19 Lockdown on air quality over the United States. *Sci. Total Environ.* 745, 141105. <https://doi.org/10.1016/j.scitotenv.2020.141105>
- Chen, N., Zhou, M., Dong, X., Qu, J., Gong, F., Han, Y., Qiu, Y., Wang, J., Liu, Y., Wei, Y., Xia, J.a., Yu, T., Zhang, X., Zhang, L. (2020b). Epidemiological and Clinical characteristics of 99 cases of 2019 novel coronavirus pneumonia in Wuhan, China: A descriptive study. *Lancet* 395, 507–513. [https://doi.org/10.1016/S0140-6736\(20\)30211-7](https://doi.org/10.1016/S0140-6736(20)30211-7)
- Cheong, K.H., Ngiam, N.J., Morgan, G.G., Pek, P.P., Tan, B.Y., Lai, J.W., Koh, J.M., Ong, M.E., Ho, A.F. (2019). Acute health impacts of the southeast Asian transboundary haze problem—A review. *Int. J. Environ. Res. Public Health* 16, 3286. <https://doi.org/10.3390/ijerph16183286>
- Collivignarelli, M.C., Abbà, A., Bertanza, G., Pedrazzani, R., Ricciardi, P., Miino, M.C. (2020). Lockdown for CoViD-2019 in Milan: What are the effects on air quality? *Sci. Total Environ.* 732, 139280. <https://doi.org/10.1016/j.scitotenv.2020.139280>
- Conticini, E., Frediani, B., Caro, D. (2020). Can atmospheric pollution be considered a co-factor in extremely high level of SARS-CoV-2 lethality in Northern Italy? *Environ. Pollut.* 261, 114465. <https://doi.org/10.1016/j.envpol.2020.114465>
- Dantas, G., Siciliano, B., França, B.B., da Silva, C.M., Arbilla, G. (2020). The impact of COVID-19



- partial lockdown on the air quality of the city of Rio de Janeiro, Brazil. *Sci. Total Environ.* 729, 139085. <https://doi.org/10.1016/j.scitotenv.2020.139085>
- Díaz-Robles, L.A., Fu, J.S., Vergara-Fernández, A., Etcharren, P., Schiappacasse, L.N., Reed, G.D., Silva, M.P. (2014). Health risks caused by short term exposure to ultrafine particles generated by residential wood combustion: A case study of Temuco, Chile. *Environ. Int.* 66, 174–181. <https://doi.org/10.1016/j.envint.2014.01.017>
- European Space Agency (ESA) (2018). Copernicus Sentinel Data Processed by ESA, Koninklijk Nederlands Meteorologisch Instituut (Knmi), Sentinel-5p Tropomi Tropospheric No2 1-Orbit L2 7km X 3.5km, Greenbelt, Md, USA, Goddard Earth Sciences Data and Information Services Center (Ges Disc). <https://doi.org/10.5270/S5P-s4ljg54>
- Faridi, S., Yousefian, F., Niazi, S., Ghalhari, M.R., Hassanvand, M.S., Naddafi, K. (2020). Impact of Sars-Cov-2 on Ambient Air Particulate Matter in Tehran. *Aerosol Air Qual. Res.* 20, 1805–1811. <https://doi.org/10.4209/aaqr.2020.05.0225>
- Finlayson-Pitts, B.J., Pitts, J.N. (2000). CHAPTER 5 - Kinetics and Atmospheric Chemistry, in: Finlayson-Pitts, B.J., Pitts, J.N. (Eds.), *Chemistry of the Upper and Lower Atmosphere*, Academic Press, San Diego, pp. 130–178. <https://doi.org/10.1016/B978-012257060-5/50007-1>
- Harapan, H., Itoh, N., Yufika, A., Winardi, W., Keam, S., Te, H., Megawati, D., Hayati, Z., Wagner, A.L., Mudatsir, M. (2020). Coronavirus disease 2019 (COVID-19): A literature review. *J. Infect. Public Health* 13, 667–673. <https://doi.org/10.1016/j.jiph.2020.03.019>
- He, G., Pan, Y., Tanaka, T. (2020). The short-term impacts of COVID-19 lockdown on urban air pollution in China. *Nat. Sustain.* 3, 1005–1011. <https://doi.org/10.1038/s41893-020-0581-y>
- Huang, M., Lin, Y., Huang, X., Liu, X., Guo, X., Hu, C., Zhao, W., Gu, X., Fang, L., Zhang, W. (2015). Experimental study of particulate products for aging of 1,3,5-trimethylbenzene secondary organic aerosol. *Atmos. Pollut. Res.* 6, 209–219. <https://doi.org/10.5094/APR.2015.025>
- Huneus, N., Urquiza, A., Gayó, E., Osses, M., Arriagada, R., Valdés, M., Álamos, N., Amigo, C., Arrieta, D., Basoa, K., Billi, M., Blanco, G., Boisier, J.P., Calvo, R., Casielles, I., Castro, M., Chahuán, J., Christie, D., Cordero, L., *et al.* (2020a). The Air We Breathe: Past, Present and Future - Air Pollution by PM<sub>2.5</sub> in Central and Southern Chile (in Spanish). Center for Climate and Resilience Research (CR)<sup>2</sup>, (ANID/FONDAP/15110009), 102 pp. <http://www.cr2.cl/contaminacion> (accessed 15 March 2020).
- Huneus, N., Denier van der Gon, H., Castesana, P., Menares, C., Granier, C., Granier, L., Alonso, M., de Fatima Andrade, M., Dawidowski, L., Gallardo, L., Gomez, D., Klimont, Z., Janssens-Maenhout, G., Osses, M., Puliafito, S.E., Rojas, N., Ccoyllo, O.S., Tolvett, S., Ynoue, R.Y. (2020b). Evaluation of anthropogenic air pollutant emission inventories for South America at national and city scale. *Atmos. Environ.* 235, 117606. <https://doi.org/10.1016/j.atmosenv.2020.117606>
- Instituto Geográfico Militar (IGM) (2013). Cartography (in Spanish). Military Geographical Institute (IGM for its acronym in Spanish). Republic of Chile. <http://www.igm.cl> (accessed 01 March 2020).
- Instituto Nacional de Estadísticas (INE) (2020). Statistical Products (in Spanish). National Institute of Statistics (INN for its acronym in Spanish), Republic of Chile. <http://www.ine.cl> (accessed 30 January 2020).
- Kanniah, K.D., Kamarul Zaman, N.A.F., Kaskaoutis, D.G., Latif, M.T. (2020). COVID-19's impact on the atmospheric environment in the Southeast Asia region. *Sci. Total Environ.* 736, 139658. <https://doi.org/10.1016/j.scitotenv.2020.139658>
- Kroll, J.H., Seinfeld, J.H. (2008). Chemistry of secondary organic aerosol: Formation and evolution of low-volatility organics in the atmosphere. *Atmos. Environ.* 42, 3593–3624. <https://doi.org/10.1016/j.atmosenv.2008.01.003>
- Kutralam-Muniasamy, G., Pérez-Guevara, F., Roy, P.D., Elizalde-Martínez, I., Shruti, V.C. (2020). Impacts of the COVID-19 lockdown on air quality and its association with human mortality trends in megapolis Mexico City. *Air Qual. Atmos. Health* 14, 553–562. <https://doi.org/10.1007/s11869-020-00960-1>
- Liu, C., Chen, R., Sera, F., Vicedo-Cabrera, A.M., Guo, Y., Tong, S., Coelho, M.S.Z.S., Saldiva, P.H.N., Lavigne, E., Matus, P., Valdes Ortega, N., Osorio Garcia, S., Pascal, M., Stafoggia, M., Scortichini, M., Hashizume, M., Honda, Y., Hurtado-Díaz, M., Cruz, J., *et al.* (2019). Ambient Particulate Air Pollution and Daily Mortality in 652 Cities. *N. Engl. J. Med.* 381, 705–715. <https://doi.org/10.1056/NEJMoa1817364>

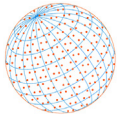


- Mahato, S., Pal, S., Ghosh, K.G. (2020). Effect of lockdown amid COVID-19 pandemic on air quality of the megacity Delhi, India. *Sci. Total Environ.* 730, 139086. <https://doi.org/10.1016/j.scitotenv.2020.139086>
- Manzano, C.A., Jácome, M., Syn, T., Molina, C., Toro, R., Leiva-Guzmán, M.A. (2020). Local air quality issues and research priorities through the lenses of Chilean experts: An ontological analysis. *Integr. Environ. Assess. Manage.* 17, 273–281. <https://doi.org/10.1002/ieam.4320>
- Mead, M.I., Castruccio, S., Latif, M.T., Nadzir, M.S.M., Dominick, D., Thota, A., Crippa, P. (2018). Impact of the 2015 wildfires on Malaysian air quality and exposure: A comparative study of observed and modeled data. *Environ. Res. Lett.* 13, 044023. <https://doi.org/10.1088/1748-9326/aab325>
- Mendez-Espinosa, J.F., Rojas, N.Y., Vargas, J., Pachón, J.E., Belalcazar, L.C., Ramírez, O. (2020). Air quality variations in Northern South America during the COVID-19 lockdown. *Sci. Total Environ.* 749, 141621. <https://doi.org/10.1016/j.scitotenv.2020.141621>
- Menut, L., Bessagnet, B., Siour, G., Mailler, S., Pennel, R., Cholokian, A. (2020). Impact of lockdown measures to combat Covid-19 on air quality over western Europe. *Sci. Total Environ.* 741, 140426. <https://doi.org/10.1016/j.scitotenv.2020.140426>
- Ministerio del Medio Ambiente (MMA) (2014). Atmospheric Decontamination Plans. Strategy 2014-2018 (in Spanish), Ministry of the Environment (MMA for its acronym in Spanish), Republic of Chile. <http://goo.gl/ulHOZf> (accessed 2 de April 2020).
- Molina, C., Toro, R., Morales S, R.G.E., Manzano, C., Leiva-Guzmán, M.A. (2017). Particulate matter in urban areas of south-central Chile exceeds air quality standards. *Air Qual. Atmos. Health* 10, 653–667. <https://doi.org/10.1007/s11869-017-0459-y>
- Nakada, L.Y.K., Urban, R.C. (2020). COVID-19 pandemic: Impacts on the air quality during the partial lockdown in São Paulo state, Brazil. *Sci. Total Environ.* 730, 139087. <https://doi.org/10.1016/j.scitotenv.2020.139087>
- National Energy Commission (CNE) (2008). Study of the Strategic Potential of Wood in the Chilean Energy Matrix (in Spanish). National Commission of Energy (CNE for its acronym in Spanish), Republic of Chile. <http://goo.gl/KKpyn8> (accessed 25 February 2021).
- National Energy Commission (CNE) (2015). Measurement of National Consumption of Firewood and Other Solid Fuels Derived from Wood (in Spanish). National Commission of Energy (CNE for its acronym in Spanish), Republic of Chile. <https://goo.gl/HQ8vzr> (accessed 14 May 2020).
- Ogen, Y. (2020). Assessing nitrogen dioxide (NO<sub>2</sub>) levels as a contributing factor to coronavirus (COVID-19) fatality. *Sci. Total Environ.* 726, 138605. <https://doi.org/10.1016/j.scitotenv.2020.138605>
- Ortega, A.M., Hayes, P.L., Peng, Z., Palm, B.B., Hu, W., Day, D.A., Li, R., Cubison, M.J., Brune, W.H., Graus, M., Warneke, C., Gilman, J.B., Kuster, W.C., de Gouw, J., Gutiérrez-Montes, C., Jimenez, J.L. (2016). Real-time measurements of secondary organic aerosol formation and aging from ambient air in an oxidation flow reactor in the Los Angeles area. *Atmos. Chem. Phys.* 16, 7411–7433. <https://doi.org/10.5194/acp-16-7411-2016>
- Otmani, A., Benchrif, A., Tahri, M., Bounakhla, M., Chakir, E.M., El Bouch, M., Krombi, M.h. (2020). Impact of Covid-19 lockdown on PM<sub>10</sub>, SO<sub>2</sub> and NO<sub>2</sub> concentrations in Salé City (Morocco). *Sci. Total Environ.* 735, 139541. <https://doi.org/10.1016/j.scitotenv.2020.139541>
- Pacheco, H., Díaz-López, S., Jarre, E., Pacheco, H., Méndez, W., Zamora-Ledezma, E. (2020). NO<sub>2</sub> levels after the COVID-19 lockdown in Ecuador: A trade-off between environment and human health. *Urban Clim.* 34, 100674. <https://doi.org/10.1016/j.uclim.2020.100674>
- Pani, S.K., Wang, S.H., Lin, N.H., Chantara, S., Lee, C.T., Thepnuan, D. (2020). Black carbon over an urban atmosphere in northern peninsular Southeast Asia: Characteristics, source apportionment, and associated health risks. *Environ. Pollut.* 259, 113871. <https://doi.org/10.1016/j.envpol.2019.113871>
- Pei, Z., Han, G., Ma, X., Su, H., Gong, W. (2020). Response of major air pollutants to COVID-19 lockdowns in China. *Sci. Total Environ.* 743, 140879. <https://doi.org/10.1016/j.scitotenv.2020.140879>
- Pino, P., Iglesias, V., Garreaud, R., Cortés, S., Canals, M., Folch, W., Burgos, S., Levy, K., Naeher, L.P., Steenland, K. (2015). Chile confronts its environmental health future after 25 years of accelerated growth. *Ann. Global Health* 81, 354–367. <https://doi.org/10.1016/j.aogh.2015.06.008>
- Punsompong, P., Pani, S.K., Wang, S.H., Bich Pham, T.T. (2021). Assessment of biomass-burning



- types and transport over Thailand and the associated health risks. *Atmos. Environ.* 247, 118176. <https://doi.org/10.1016/j.atmosenv.2020.118176>
- Python (2020). Python Software Foundation. Python Language Reference, Version 2.7. <http://www.python.org> (Accessed 25 March 2021).
- R Core Team (2020). R: A Language and Environment for Statistical Computing. R Foundation for Statistical Computing, Vienna, Austria. <http://www.r-project.org/> (accessed 10 March 2020).
- R StudioTeam (2020). Integrated Development for R. Rstudio, Inc. <http://www.rstudio.com> (accessed 1 October 2020).
- Represa, N.S., Della Ceca, L.S., Abril, G., García Ferreyra, M.F., Scavuzzo, C.M. (2021). Atmospheric pollutants assessment during the COVID-19 lockdown using remote sensing and ground-based measurements in Buenos aires, Argentina. *Aerosol Air Qual. Res.* 21, 200486. <https://doi.org/10.4209/aaqr.2020.07.0486>
- Rojas, J.P., Urdanivia, F.R., Garay, R.A., García, A.J., Enciso, C., Medina, E.A., Toro, R., Manzano, C., Leiva-Guzmán, M.A. (2021). Effects of COVID-19 pandemic control measures on air pollution in Lima metropolitan area, Peru in South America. *Air Qual. Atmos. Health* 14, 925–933. <https://doi.org/10.1007/s11869-021-00990-3>
- Sanità di Toppi, L., Sanità di Toppi, L., Bellini, E. (2020). Novel coronavirus: How atmospheric particulate affects our environment and health. *Challenges* 11, 6. <https://doi.org/10.3390/challe11010006>
- Sbai, S.E., Farida, B. (2019). Photochemical aging and secondary organic aerosols generated from limonene in an oxidation flow reactor. *Environ. Sci. Pollut. Res.* 26, 18411–18420. <https://doi.org/10.1007/s11356-019-05012-5>
- Sbai, S.E., Mejjad, N., Norelyaqine, A., Bentayeb, F. (2021). Air quality change during the COVID-19 pandemic lockdown over the Auvergne-Rhône-Alpes region, France. *Air Qual. Atmos. Health* 14, 617–628. <https://doi.org/10.1007/s11869-020-00965-w>
- Seguel, R.J., Gallardo, L., Osses, M., Rojas, N.Y., Landulfo, E., Andrade, M., Nogueira, T., Rondanelli, R., Huneeus, N., Menares, C., Fleming, Z.L., Mangones, S., Eskes, H., Belalcázar, L.C., Rojas, J.P., Ibarra-Espinosa, S., Munizaga, M., Pantoja, N., Carrasco, P., *et al.* (2020). Primary and secondary air pollutant response during the Covid-19 lockdown in south American megacities: Learning about present and future air quality. 2020. submitted.
- Sharma, S., Zhang, M., Anshika, Gao, J., Zhang, H., Kota, S.H. (2020). Effect of restricted emissions during COVID-19 on air quality in India. *Sci. Total Environ.* 728, 138878. <https://doi.org/10.1016/j.scitotenv.2020.138878>
- Shehzad, K., Sarfraz, M., Shah, S.G.M. (2020). The impact of COVID-19 as a necessary evil on air pollution in India during the lockdown. *Environ. Pollut.* 266, 115080. <https://doi.org/10.1016/j.envpol.2020.115080>
- Sicard, P., De Marco, A., Agathokleous, E., Feng, Z., Xu, X., Paoletti, E., Rodriguez, J.J.D., Calatayud, V. (2020). Amplified ozone pollution in cities during the COVID-19 lockdown. *Sci. Total Environ.* 735, 139542. <https://doi.org/10.1016/j.scitotenv.2020.139542>
- Sistema de Información Nacional de Calidad del Aire (SINCA) (2020). National Air Quality System on Line System (in Spanish). Ministry of the Environment, Republic of Chile, Santiago. <http://sinca.mma.gob.cl> (accessed 10 June 2020).
- State of Global Air (SGA) (2020). State of Global Air 2020 Health Effects Institute and the Institute for Health Metrics and Evaluation's. <https://www.stateofglobalair.org/data/#/health/plot> (accessed 25 February 2021).
- Tian, J., Wang, Q., Zhang, Y., Yan, M., Liu, H., Zhang, N., Ran, W., Cao, J. (2021). Impacts of primary emissions and secondary aerosol formation on air pollution in an urban area of China during the COVID-19 lockdown. *Environ. Int.* 150, 106426. <https://doi.org/10.1016/j.envint.2021.106426>
- Tobías, A., Carnerero, C., Reche, C., Massagué, J., Via, M., Minguillón, M.C., Alastuey, A., Querol, X. (2020). Changes in air quality during the lockdown in Barcelona (Spain) one month into the SARS-CoV-2 epidemic. *Sci. Total Environ.* 726, 138540. <https://doi.org/10.1016/j.scitotenv.2020.138540>
- Toro, R., Morales S, R.G.E., Canales, M., Gonzalez-Rojas, C., Leiva-Guzmán, M.A. (2014). Inhaled and inspired particulates in Metropolitan Santiago Chile exceed air quality standards. *Build. Environ.* 79, 115–123. <https://doi.org/10.1016/j.buildenv.2014.05.004>





- Toro, R., Campos, C., Molina, C., Morales S, R.G.E., Leiva-Guzmán, M.A. (2015). Accuracy and reliability of Chile's National Air Quality Information System for measuring particulate matter: Beta attenuation monitoring issue. *Environ. Int.* 82, 101–109. <https://doi.org/10.1016/j.envint.2015.02.009>
- Toro, R., Kvakić, M., Klaić, Z.B., Koračin, D., Morales S, R.G.E., Leiva-Guzmán, M.A. (2019). Exploring atmospheric stagnation during a severe particulate matter air pollution episode over complex terrain in Santiago, Chile. *Environ. Pollut.* 244, 705–714. <https://doi.org/10.1016/j.envpol.2018.10.067>
- Toro, R., Catalan, F., Urdanivia, F.R., Rojas, J.P., Manzano, C., Seguel, R., Gallardo, L., Osses, M., Pantoja, N., Leiva-Guzmán, M.A. (2021). Air pollution and COVID-19 lockdown in a large South American city: Santiago Metropolitan Area, Chile. *Urban Clim.* 36, 100803. <https://doi.org/10.1016/j.uclim.2021.100803>
- Wu, X., Nethery, R.C., Sabath, B.M., Braun, D., Dominici, F. (2020). Air pollution and COVID-19 mortality in the United States: Strengths and limitations of an ecological regression analysis. *Sci. Adv.* 6, eabd4049. <https://doi.org/10.1126/sciadv.abd4049>
- Zalakeviciute, R., Vasquez, R., Bayas, D., Buenano, A., Mejia, D., Zegarra, R., Diaz, V., Lamb, B. (2020). Drastic improvements in air quality in Ecuador during the COVID-19 outbreak. *Aerosol Air Qual. Res.* 20, 1783–1792. <https://doi.org/10.4209/aaqr.2020.05.0254>
- Zhang, R., Wang, G., Guo, S., Zamora, M.L., Ying, Q., Lin, Y., Wang, W., Hu, M., Wang, Y. (2015). Formation of urban fine particulate matter. *Chem. Rev.* 115, 3803–3855. <https://doi.org/10.1021/acs.chemrev.5b00067>
- Zhang, Z., Xue, T., Jin, X. (2020). Effects of meteorological conditions and air pollution on COVID-19 transmission: Evidence from 219 Chinese cities. *Sci. Total Environ.* 741, 140244. <https://doi.org/10.1016/j.scitotenv.2020.140244>